



HHS Public Access

Author manuscript

Mitochondrion. Author manuscript; available in PMC 2020 November 01.

Published in final edited form as:

Mitochondrion. 2019 November ; 49: 217–226. doi:10.1016/j.mito.2019.09.005.

Fis1 deficiencies differentially affect mitochondrial quality in skeletal muscle

Zhe Zhang^{1,2,3}, Danielle A. Sliter², Christopher K. E. Bleck⁴, Shuzhe Ding^{1,3}

¹The Key Laboratory of Adolescent Health Assessment and Exercise Intervention, Ministry of Education, East China Normal University, Shanghai 200241, China

²Biochemistry Section, Surgical Neurology Branch, National Institute of Neurological Disorders and Stroke, National Institutes of Health, Bethesda, Maryland 20892, USA

³School of Physical Education and Health care, East China Normal University, Shanghai 200241, China

⁴Electron Microscopy Core Facility, National Heart, Lung, and Blood Institute (NHLBI) Bethesda, National Institutes of Health, United States

Abstract

Mitochondrial dynamics and mitophagy are important aspects of mitochondrial quality control, and are linked to neurodegenerative diseases and muscular diseases. Fis1, a protein on the mitochondrial outer membrane, is thought to mediate mitochondrial fission. However, Fis1 null worms and mammalian cells only display mild fission defects but show aberrant mitophagy. To assess Fis1 function *in vivo*, we generated conditional knock-out Fis1 mice to allow for specific Fis1 deletion in adult skeletal muscle. In the absence of Fis1 in Type I muscle, mitochondrial hyperfusion, respiratory chain deficiency, and increased mitophagy were found. Moreover, abnormal mitophagy was aggravated by endurance exhaustive exercise stress (EEE), suggesting that Fis1 is involved in maintaining normal mitophagy in mitochondria-rich Type I muscle during exercise. Additionally, Fis1 loss induced delayed onset muscle ultrastructure change (DOMUC) in Type I muscle and strong inflammation in response to acute exhaustive exercise (EE). Thus, we identify a role for Fis1 in maintaining normal mitochondrial structure and function at rest and under exercise stress.

Keywords

Fis1; mitochondrial dynamics; mitophagy; inflammation response; exhaustive exercise

Author Contributions

Z.Z. planned, performed experiments and wrote the manuscript. D.A.S. performed blood collection, EE, body temperature analysis and edited the manuscript. C.K.E.B. performed Immuno-EM experiments. L.H. reviewed the manuscript. S.D. edited the manuscript.

Declaration of Interests

The authors declare no competing interests.

Publisher's Disclaimer: This is a PDF file of an unedited manuscript that has been accepted for publication. As a service to our customers we are providing this early version of the manuscript. The manuscript will undergo copyediting, typesetting, and review of the resulting proof before it is published in its final form. Please note that during the production process errors may be discovered which could affect the content, and all legal disclaimers that apply to the journal pertain.

Introduction

Mitochondria are the organelles that provide energy in the form of adenosine triphosphate (ATP) to the cell. Mitochondria constantly fuse and divide within cells; a process called mitochondrial dynamics. Mitochondrial fission and fusion play critical roles in maintaining functional mitochondria when cells experience metabolic or environmental stresses. Fusion helps mitigate stress by mixing the contents of partially damaged mitochondria as a form of complementation. Fission is needed to create new mitochondria, and can regulate mitochondria by allowing the removal of damaged mitochondria during cellular stress through a selective autophagic process called mitophagy.¹ Disrupting mitochondrial dynamics and mitophagy can affect normal development, and has been implicated in neurodegenerative diseases, such as Parkinson's disease, Alzheimer's disease and the muscle wasting disease, sarcopenia (muscle deterioration).²⁻⁴ Therefore, mitochondrial dynamics and mitophagy together keep the mitochondrial pool healthy and suggest that pharmacologically or genetically restoring normal mitochondrial dynamics could be therapeutic to alter the course of these diseases.

Mitochondrial fission and fusion processes are mediated by large guanosine triphosphatases (GTPases) in the dynamin family that are well conserved between yeast, flies, and mammals.⁵ In mammals, fusion between mitochondrial outer membranes is mediated by Mfn1 and Mfn2, whereas fusion between mitochondrial inner membranes is mediated by Opa1.⁵ Fission is mediated by a cytosolic dynamin family member Drp1. Drp1 is recruited from the cytosol to the mitochondria to form spirals around mitochondria that constrict to sever both inner and outer membranes. Upon mitochondria damage, the protein PINK1 is stabilized on the outer mitochondrial membrane where functions to recruit and activate Parkin to induce mitophagy.^{7,8} Mitophagy can be inhibited by a dominant negative mutant of Drp1, suggesting that fission is required for mitophagy.⁹

Fis1, is also thought to mediate mitochondrial fission. Fis1 was first discovered in yeast, in which it is the sole Drp1 recruitment factor.¹⁰ Fis1 which resides on the mitochondrial outer membrane, has two TPR motifs that bind to the yeast Drp1 homologue Dnm1 through adaptor proteins.¹¹⁻¹⁵ Fis1 is present throughout the animal kingdom, but its function in metazoans is unclear. Fis1 can bind to human Drp1 *in vitro*, can promote fission when overexpressed, and has been implicated in a number of fission dependent processes, such as apoptosis and autophagy.^{9,16-20} However, mammalian Fis1 knockout cells have mild or no fission defects,^{21,22} suggesting that Fis1 plays an ancillary role in this process. Furthermore, it was recently reported by our group that Fis1 null worms and Fis1 knockout mammalian cells have excessive LC3 accumulation following stress induced by mitochondrial toxins,^{7,10} indicating Fis1 may have a role in mitophagy. To date, there is no literature on the role of mammalian Fis1 *in vivo* (be it dynamics or mitophagy).

Systemic knock out Fis1 is lethal for mice, therefore to understand the function of Fis1 *in vivo*, we generated a conditional knockout mouse model (Fis1^{fl/fl}) which were cross-bred with MCK-Cre transgenic mice to allow skeletal muscle-specific deletion (Fis1^{fl/fl} X MCK-Cre, Fis1KO) to examine mitochondrial function. Skeletal muscle is highly reliant on mitochondrial dynamics for proper mitochondrial function, especially during exercise, and

change in mitochondrial quality and function is necessary for proper muscle development.²³ We found that loss of Fis1 caused mitochondrial hyperfusion, impaired mitochondrial function, and also resulted in abnormal mitophagy in Type I muscle fibers, especially under endurance exercise stress. Furthermore, we found that Fis1KO exacerbated DOMUC in Type I muscle and induced inflammation following intensive exercise stress. Together, our results indicate a role for Fis1 in mitochondrial quality control *in vivo* at rest and under exercise stress.

Results

Loss of Fis1 leads to abnormal mitochondrial morphology in skeletal muscles

To generate conditional Fis1 knockout mice, exons 2–4 of Fis1 were flanked by loxP sites (Fig. 1A), then cross-bred with the MCK-Cre transgenic mice to allow myoblast-specific deletion in skeletal muscle. We confirmed loss of Fis1 protein in soleus, gastrocnemius and quadriceps (Fig. 1B), but not that in heart and liver (Fig. S1A). Ultrastructural examination of mitochondria appeared largely unchanged in Fis1KO versus wild-type (WT) quadriceps (Fig. 1C) through electron microscope (EM). However, mitochondria are enlarged in Fis1KO soleus compared with WT soleus (Fig. 1C and D). We also found more swollen mitochondria characterized by loss of cristae and a low matrix density in Fis1KO gastrocnemius compared with WT gastrocnemius (Fig. 1C and E, $P=0.06$). Despite alterations in mitochondrial morphology, the skeletal muscle structure did not change (Fig. S1B).

Loss of Fis1 impairs mitochondrial respiratory chain in slow muscle

Expression of respiratory chain complexes and the histochemical staining of muscle cryosections for reduced form of nicotinamide-adenine dinucleotide (NADH) can reveal mitochondrial oxidative phosphorylation (OXPHOS) alterations. To assess the mitochondrial function, we measured the expression level of mitochondrial OXPHOS complexes I–V, in soleus, gastrocnemius and quadriceps muscle lysates prepared from 12-week-old WT and Fis1KO mice by immunoblotting (Fig. 2A, Fig. S1C and D). These analyses revealed that only the protein level of Complex I (CI-NDUFB8) was significantly reduced in Fis1KO soleus (Fig. 2A and B), with no differences observed among any OXPHOS complexes in Fis1KO gastrocnemius or quadriceps (Fig. S1C and D). Consistent with the former finding, Complex I activity decreased in soleus of Fis1 KO mice ($P=0.05$) (Fig. 2C). On the other hand, gastrocnemius and soleus muscle sections derived from 12-week-old WT and Fis1KO mice were stained for reduced NADH, which also reflects Complex I function. Consistent with immunoblotting, we observed less NADH signal in Fis1KO compared to WT soleus; the overall intensity of NADH in the interior of the fiber appeared drastically reduced, so called rubbed-out fibers²⁴ (Fig. 2D) and no differences between Fis1KO and WT gastrocnemius were observed (Fig. 2E). Therefore, Fis1KO decreased mitochondrial respiratory capacity via Complex I in soleus.

Excessive GFP-LC3 is exacerbated in Fis1-deficient soleus through endurance exhaustive exercise (EEE)

Since we found enlarged, elongated and swollen mitochondria in Fis1KO soleus and gastrocnemius respectively, and reduced Complex I expression in soleus, we hypothesized that this may cause exercise intolerance due to reduced energy production.²⁵ To test this, we performed a sprint test on a treadmill. Here, after acclimation to the treadmill, mice were forced to run at 14m/min for 5 minutes and the number of times a mouse fell off the rear of the treadmill were counted as a readout of endurance.²⁶ Fis1KO mice fell significantly more times than WT mice during the test, suggesting that loss of Fis1 in skeletal muscle impairs mice endurance exercise ability (Fig. 3A).

Given that Fis1 may play a role in mitophagy and autophagy and that Fis1KO can result in aberrant LC3 accumulation during mitophagy,^{7,10,27} we crossed the skeletal muscle specific Fis1KO mice with mice transgenically overexpressing GFP-LC3, a marker of autophagosomes, in order to analyze autophagy in tissues of Fis1KO mice by confocal microscopy. Similar with previous reports,^{7,10} Fis1KO resulted in increased GFP-LC3 puncta in soleus of sedentary mice compared to WT mice (Fig. 3B and C).

As treadmill running is reported to induce autophagy and mitophagy,²⁷ we used the running paradigm (referred to as endurance exhaustive exercise (EEE)) to assess GFP-LC3 accumulation in WT and Fis1KO muscle. This exercise paradigm is mainly for aerobic exercise, in which we let the mice run slower and longer to allow mitochondria contribute more during this stress process. Following EEE, there was no significant change in GFP-LC3 puncta in soleus from WT mice, however, GFP-LC3 further increased in Fis1-deficient soleus compared with Fis1KO sedentary (SED) mice and WT mice (Fig. 3B and C). There were no changes in GFP-LC3 of gastrocnemius in either genotype, even after EEE (Fig. 3D and E). To clarify the nature of LC3 accumulation in Fis1KO soleus in more detail, we conducted immunoelectron microscopy to analyze autophagosomes. EEE caused the normal formation of autophagosomes with closely apposed membranes that were labeled with gold particle attached to GFP-LC3 near mitochondria in WT-GFP-LC3 soleus (Fig. 3F). Although Fis1KO-GFP-LC3 soleus has similar autophagosomes' structure (Fig. 3Ga), many of them displayed disordered distribution and LC3 aggregation that contain mitochondria and possibly other organelles (Fig. 3Gb), which is consistent with previous findings.⁷

Acute Exhaustive Exercise (EE) is followed by inflammation response in Fis1^{-/-} muscle and blood

Mitochondrial stress induced by acute exhaustive exercise (EE) can lead to the release of damage-associated molecular patterns that activate innate immunity in mice that lack intact mitophagy pathways, while WT mice have no response.²⁸ In this exercise paradigm, failure of mitochondrial clearance following EE resulted in increased cytokines in the blood and increased body temperature that correlated with cytokine increases.²⁸ Given our finding that loss of Fis1 may alter mitochondrial clearance *in vivo* in soleus in response to EEE, we sought next to determine how loss of Fis1 may impact the inflammatory response to EE. For this 10–12-week old Fis1KO mice were exercised until exhausted for three consecutive days. We monitored changes in body temperature and circulating plasma cytokines before, during,

and after exercise. Average time to exhaustion (Fig. S2A) and baseline cytokine levels in Fis1KO mice were similar to those of WT (Fig. 4B). Body temperature remained constant in WT animals throughout the trial, as previously reported²⁸ (Fig. S2B). Interestingly, compared with Fis1KO sedentary mice, we found that the body temperature of the Fis1KO mice subjected to EE increased significantly on trial day 16, two days after the EE trial, and remained elevated until trial day 20 (Fig. 4A). In addition, plasma cytokines remained at baseline in WT mice after EE, but loss of Fis1 in skeletal muscle led to a significant increase in plasma cytokines (IL-6, IL-12p40, IL-13, KC, RANTES and IFN β) immediately after the EE trial (Fig. 4B). 6 days after EE, all cytokine levels returned to baseline, indicating that similar to EE in mice that lack mitophagy pathways,²⁸ loss of Fis1 in skeletal muscle induces a robust, but acute, inflammatory response.

In consideration of our mice model is specific knock out Fis1 in skeletal muscle, we wondered whether the inflammatory response in skeletal muscle was also increased. Soleus and gastrocnemius muscle sections were prepared from 12-week-old WT and Fis1KO SED or EE mice and analyzed by confocal microscopy for the macrophage specific antigen F4/80. Interestingly, we found increased F4/80 in Fis1KO gastrocnemius but not WT after EE, and no changes in F4/80 in soleus of either genotype (Fig. 4C and D).

EE exacerbates delayed onset muscle ultrastructure change (DOMUC) and swollen mitochondria in Fis1-deficient slow and quick muscle respectively

Macrophages are a type of white blood cell, of the immune system, that engulfs and digests cellular debris, foreign substances, microbes, cancer cells, and anything else that does not have the type of specific antigen to healthy body cells on its surface in a process called phagocytosis.²⁹ Hence macrophage is an important index of tissue damage and inflammation. Moreover, tissue damage can also induce inflammatory response. In view of macrophages and cytokines' level, we wondered if EE induce muscle damage. Soleus and gastrocnemius muscle were prepared for EM 12–24h after the EE trial. We found that EE resulted in large-scale ultra-structure damage in Fis1KO soleus, with Z-band disorganized and broadened, showing typical delayed onset muscle ultrastructure change (DOMUC) (Fig. 5A). There was no obvious ultrastructural change in the gastrocnemius after EE, however, more swollen mitochondria were observed in FIS1KO than WT (Fig. 5B and C). Thus, increased macrophage found in gastrocnemius may relate to the increase in swollen mitochondria rather than structural changes in tissue.

Since the EM images showed obvious damage in Fis1-deficient soleus, we investigated the level of creatine kinase (CK) in the blood. CK catalyzes the conversion of creatine and utilizes ATP to create phosphocreatine (PCr) and adenosine diphosphate (ADP). This CK enzyme reaction is reversible and thus ATP can be generated from PCr and ADP.³⁰ Clinically, CK is assayed in blood tests as a marker of damage of CK-rich tissue for conditions such as rhabdomyolysis (severe muscle breakdown), myocardial infarction (heart attack), muscular dystrophy and autoimmune myositides.³¹ Consistent with our predictions, we found CK levels are similar between WT and Fis1KO mice at baseline, however, immediately after EE, the level of CK in Fis1KO mice increased significantly while WT levels remained at baseline (Fig. 5D). Unexpectedly, on the 6th day after running, while

cytokines had returned to baseline, the CK level of Fis1KO remained elevated (Fig. 5D), consistent with the observed damage in Fis1KO soleus. We speculated that loss of Fis1 lead to serious DOMUC following EE in soleus resulting in significantly elevated CK.

Discussion

In conclusion, the present study provides new insights into the *in vivo* function of mammalian Fis1. We describe, for the first time, an *in vivo* role for Fis1 in maintaining normal mitochondrial function and morphology. We report increased LC3 puncta in skeletal muscle at rest and after exercise challenge, indicating a link between Fis1 activity and autophagy and mitophagy. Finally, we also find a role for Fis1 in responding to mitochondrial stress induced by exercise, by preventing increased muscle damage and inflammation, and limiting DOMUC.

Alterations in mitochondrial morphology induced by loss of Fis1 occurred in soleus. Our images showed that loss of Fis1 results in mitochondrial hyper-fusion in soleus (Fig. 1C and D) and swollen mitochondria ($P=0.06$) in the gastrocnemius (Fig. 1C and E), with no consequence in the quadriceps. Similar with our observation, heart-specific knockout of Mfn1, Mfn2 and Drp1, also resulted in the appearance of swollen mitochondria characterized by mitochondrial matrix disappearance ($P < 0.05$).³² Furthermore, overexpression of Drp1 reduced mitochondrial area and swelling in the tibialis anterior muscle,²³ indicating that perturbations in mitochondrial structure are a common phenomenon when mitochondrial dynamics are impaired.

Furthermore, we observed that Fis1KO soleus had impaired OXPHOS capacity, and a significant decrease in the Complex I function (Fig. 2A, B and C). However, in gastrocnemius and quadriceps, there was no change in the expression of OXPHOS Complexes (Fig. S1C and D). Consistent with the observed defects in OXPHOS, indicating mitochondrial dysfunction, we observed an increase GFP-LC3 puncta in Fis1KO soleus *in vivo*, suggesting that loss of Fis1 in type I muscle fibers can result in mitophagy induction to clear damaged mitochondria (Fig. 3B and C). In support of this, there are no increases in GFP-LC3 in gastrocnemius and quadriceps where no alterations in OXPHOS were observed (Fig. 3D and E). Thus, although the mechanism remains unclear, our data indicate that *in vivo* Fis1 functions in mitochondrial dynamics, and that its loss has different consequences in different muscle types.

We speculated that these muscle specific differences were due to the different types of muscle fibers that comprise each muscle. Skeletal muscle can be divided into red slow muscle (type I) and white fast muscle (type II) according to different functional characteristics. Type I muscle fiber has thinner fibers, less myofibrils, more mitochondria and myoglobin, smaller dominating neurons, abundant peripheral capillaries, higher oxidase activity, and higher activity of glycolytic enzymes, slower contraction, less contraction strength, but longer duration and less fatigue than type II muscle fiber²³. The soleus is composed predominately of type I muscle fibers, the gastrocnemius is composed predominately of type II muscle fibers and the quadriceps contain an equal proportion of both type I and type II fibers.³³ Thus, the soleus, which is mitochondria-rich, may be more

susceptible to the loss of Fis1, as supported by the observed decreased Complex I, OXPHOS and by increased GFP-LC3.

The enlarged mitochondria and OXPHOS deficits observed in Fis1KO soleus, could impair energy production, substrate and oxygen delivery and exchange, and contribute to exercise intolerance.²⁵ Indeed, using a sprint endurance test we found that Fis1KO mice displayed a significant reduction in endurance capacity compared to WT (Fig. 3A). Furthermore, increased GFP-LC3 was observed in Fis1KO soleus after EEE compared to WT (Fig. 3B and C), however, immune-EM revealed irregular GFP-LC3 particle distribution and accumulation (Fig. 3Gb). We found knocking out Fis1 induced abnormal mitophagy, and our results suggested many of the autophagosomes' structure displayed disordered distribution and LC3 aggregation that contain mitochondria and possibly other organelles following EEE. This suggests that EEE may induce mitophagy, but Fis1 loss may impair the execution of mitophagy, which is similar to the findings of Yamano et al.⁷ On the other hand, mutations in Fis1 do not increase the total amount of mitophagy or affect mitophagy at later stages *in vitro*. It seems likely that the total number of mitochondria that enter the mitophagy pathway remains the same. However, mutations in Fis1 slow the disposal process at a stage before fusion to lysosomes, causing a temporary buildup of intermediates in the disposal pathway and resulting in LC3/LGG-1 aggregates.¹⁰ This is also probably the mechanism in LC3 aggregation *in vivo*. Furthermore, our team already showed that Fis1 acts at a critical junction in major stress response pathways. Depending on the stress conditions, Fis1 can contribute to apoptosis or to the orderly disposal of defective mitochondria through mitophagy,¹⁰ which may be the role of Fis1 in mitophagy *in vivo*.

Utilizing EE, we found that following EE, Fis1KO mice, but not WT mice, displayed a dramatic increase in both body temperature and pro-inflammatory plasma cytokines (IL-6, IL-12p40, IL-13, KC, RANTES and IFN β) ($P < 0.001$) (Fig. 4A and B). These results indicate strong inflammation response in Fis1KO mice following EE, consistent with the level of cytokines. The time lag between body temperature rise and the increase of cytokines is also consistent with the finding in Sliter *et al.*²⁸. Interestingly, we observed increased infiltration of macrophage cells into gastrocnemius muscle following EE, but not in soleus, highlighting another muscle fiber type specific difference in the loss of Fis1 (Fig. 4C and D). More swollen mitochondria were found in Fis1KO gastrocnemius after EE compared to WT (Fig. 5B and C), but we did not observe increased mitophagy following exercise in gastrocnemius. Thus, we speculate, similar to previous reports, that EE increases mitochondrial stress, as evidenced by increased swollen mitochondria, which can induce inflammation. So while mitophagy was not observed in gastrocnemius following a more mild exercise regime (Fig. 3D and E), here EE-induced inflammation may arise from the Type II muscle fibers acting as an endocrine-like organ.³⁴

Interestingly, plasma CK levels were also significantly elevated following EE in Fis1KO but not WT mice, indicating significant muscle damage. H&E staining (Fig. S2C) and electron microscopy (Fig. 5A) images of soleus from the two groups of mice collected 12 hours after EE, revealed large ultrastructural changes in the soleus of Fis1KO mice, showing the typical phenomenon of delayed onset muscle ultrastructure change (DOMUC), which can also called delayed onset muscle soreness (DOMS). Friden et al.,³⁵ indicates that the

disturbances in ultrastructure of muscle fiber normally emerge immediately after eccentric exercise, peak is on the third day after exercise, and return to normal on the sixth day. These results support the muscle damage theory of DOMS, first described in 1902 by Theodore Hough, which concluded that soreness is “fundamentally the result of ruptures within the muscle”.^{36,37} According to this “muscle damage” theory of DOMS, these ruptures are microscopic lesions at the Z-line of the muscle sarcomere.³⁷ Taken together therefore, we speculate that lacking in Fis1 exacerbates the DOMUC in Type I muscle fibers after EE, which leads to high level of CK in the blood.

Data supporting these concepts are still preliminary, and further investigations are necessary to elucidate the precise role of Fis1 in mitochondrial quality control *in vivo*. Future experiment is needed to confirm that the changes of mitochondrial morphology is due to the changes of protein expression that related to mitochondrial dynamics. While loss of Fis1 increased GFP-LC3 puncta in sedentary and exercised animals, it is unclear whether this observation indicates a failure to fully clear damaged mitochondria or an increase in the rate of mitophagy *in vivo*. While many *in vitro* studies support a role for Fis1 in the execution of mitophagy, more work needs to be done to clarify this point *in vivo*. Furthermore, the interaction of STX17 and Fis1 is a PINK1-Parkin-independent mitophagy process.³⁸ This is also an important issue for our work. Abnormal mitophagy is linked with neuronal and cardiovascular diseases, thus it is necessary to define the accurate role of Fis1 and its association with mitophagy in various tissues, such as in brain, and to what extent does Fis1 affect human pathology. Our team has already found that Fis1 is associated with Pink1-Parkin dependent mitophagy *in vitro*,^{7,10} thus future efforts will be aimed at examining Fis1 within the context of Pink1/Parkin loss. Finally, the molecular mechanisms leading to the various phenotypes observed in different muscle types under diverse stress in the absence of Fis1 remain to be elucidated and understanding these mechanisms could be valuable to unveil the effects of mitochondrial dysfunction at disease states. In summary, our work, for the first time, described *in vivo* phenotypes related to the loss of Fis1, which is critical to maintain mitochondrial quality control and integrity.

Material and Methods

Animals

All mice were housed in pathogen-free facilities under 12-hr light dark cycles with access to food and water ad libitum. The Fis1^{FL/FL} mouse was obtained from inGenious Targeting Laboratory (iTL). The conditional loss-of-function mouse model was generated by targeting exons 2–4 of Fis1 with loxP sites. Targeted iTL IC1 (C57BL/6) embryonic stem cells were microinjected into Balb/c blastocysts. Resulting chimeras with a high percentage black coat color were mated to C57BL/6 FLP mice to remove the Neo cassette. MCK-cre model was obtained from Jackson Laboratories. Fis1^{fl/fl} mice were cross-bred with the MCK-Cre transgenic model to allow myoblast-specific deletion in the adult skeletal muscle. All mice have the nuclear background of C57BL/6J. All animal studies were carried out as approved by the Animal Care and Use Committee of the National Institute for Neurological Disorders and Stroke. The mice genotype was confirmed through PCR (NDEL, Cre, GFP-LC3) and western blot.

Antibodies

For immunoblotting, immunofluorescence microscopy and immune-electronic microscopy, the following primary antibodies were used: rabbit monoclonal antibodies to Fis1 (ALEXIS, ALX-210–1037-0100), to GAPDH (Abcam, ab8245), to Tom20 (Santa Biotechnology, sc-11415) and to GFP (Rockland, 600–401-215) and mouse monoclonal antibodies to OXPHOS (Abcam, ab110413), to tublin (Sigma-Aldrich, T9026), and to F4/80 (BM8) (Invitrogen, 13–4801-81). For immunoblot analyses, primary antibodies were used in combination with HRP-conjugated secondary antibodies (Sigma-Aldrich).

Preparation of tissue lysates

Tissue lysates for western-blot analyses were prepared as described.³⁹ All protein samples were lysed by homogenization in RIPA lysis buffer with protease inhibitors (Roche), left on ice for 15 minutes, sonicated and centrifuged max speed 4 degrees for 10 minutes. The supernatant was collected and protein concentration was measured using the DC protein assay kit (BioRad). Samples were separated on NuPAGE Novex 8%–12% Bis-Tris gels (Thermo Fisher) using 1 x MOPS or 1 x MES Running buffer (Thermo Fisher). Proteins were transferred to PVDF membranes (Bio-Rad). 5% skim milk and 3% BSA in PBS-T were used for blocking and diluting antibodies respectively.

Preparation for EM

The relevant muscle was stretched and collected in a puddle of fixation buffer (4% formaldehyde, 2.5% glutaraldehyde in 0.1 M sodium cacodylate buffer, pH 7.4). A JEOL electron microscope (JEM-1400, JEOL, Tokyo, Japan) at 1,500x - 5,000x direct magnifications was used for ultrastructural examination of osmium tetroxide/uranyl acetate stained skeletal muscle thin sections (90 nm). Image J was used on transmission electron microscopic images for measuring individual mitochondrial size and the percentage of swollen mitochondria.

Complex I Activity

Complex I activity were measured as previously described.⁴⁰ Mitochondria were extracted from skeletal muscle, mitochondrial membranes were disrupted first by freeze–thawing the samples two or three times in hypotonic medium (25 mM K₂PO₄ pH 7.2, 5 mM MgCl₂) followed by a hypotonic shock in H₂O.⁴² Using 50mM Tris medium, 0.8mM NADH as donor, 240μM KCN and rotenone to test Complex I activity.

Histochemistry of frozen tissue sections

Skeletal muscle was snap-frozen in isopentane cooled with liquid nitrogen. NADH staining of frozen sections (10 μm) were performed as described in Reference.²⁴ H & E, Sirius red, and toluidine blue staining were performed using standard procedures. Samples were recorded using Widefield microscope (Zeiss LSM510). Images were analyzed using Image J software.

Quantification of GFP-LC3 signal

Thin sections (10 μ m) from skeletal muscle were snap-frozen in isopentane cooled with liquid nitrogen. The images were captured with LSM510 confocal microscope (Carl Zeiss, Inc.) and processed using the LSM Image Browser (generation of projections of confocal stacks; Carl Zeiss, Inc.) and Photoshop CS2 (brightness and contrast adjustments; Adobe, USA). The number of GFP-LC3 puncta per unit area of tissue was quantified as described.⁴³

Immunoelectron microscopy

Fis1KO anti-GFP-LC3 tissue sample were fixed in 4% formaldehyde, 0.1% glutaraldehyde (GA) in 60 mM PIPES, 25 mM HEPES, 10 mM EGTA, and 1 mM MgCl₂ (pH 6.9) (PHEM buffer, pH 6.9)⁴⁴ for 90 min. After 5 min supernatant was removed and replaced with a freshly prepared fixative. Tissue was carefully mixed in 10% gelatin/PBS, incubated for 10–20 min at 37°C, and immediately placed on ice until the gelatin was hardened. Sample was cut into sub 1 mm³ pieces. Gelatin-embedded samples were infiltrated with 2.3 M sucrose (in 0.1 M phosphate buffer) and put at 4°C overnight on a rotating wheel, mounted onto sample pins and plunge-frozen in liquid nitrogen.

Cryosectioning and immunolabeling were performed as described.^{45,46} In brief, ultrathin sections (50–60 nm) from gelatin-embedded and frozen tissue were obtained using an FC7/UC7-ultramicrotome (Leica, Austria).

Immunogold labelling was carried out on thawed sections with an anti-GFP antibody (1:200, Rockland, Gilbertsville, PA, USA) and 10 nm protein A-gold (1:50, UMC Utrecht University, Utrecht, The Netherlands) as described,^{46,47} and stained/embedded in 4% uranyl acetate / 2% methylcellulose mixture (ratio 1:9).⁴⁸ Thin sections were examined on a JEM-1200EX (JEOL USA) transmission electron microscope (accelerating voltage 80 keV) equipped with an AMT 6-megapixel digital camera (Advanced Microscopy Techniques Corp, USA).

Immunofluorescence microscopy

Thin sections (10 μ m) from skeletal muscle were snap-frozen in isopentane cooled with liquid nitrogen. Slides were fixed with 4% PFA, permeabilized with 0.15% Triton X-100, blocked with 5% BSA for 1 hr at room temperature (RT) and incubated with F4/80 Antibody (BM8) (Invitrogen 13–4801-81) at 1:100, and DAPI (Sigma Aldich D9542) at 1:500. Slides were then mounted with fluorescent mounting media with DAPI (Vector Laboratories). Images were captured using a LSM510 confocal microscope (Carl Zeiss, Inc.) and processed using the LSM Image Browser (generation of projections of confocal stacks; splitting of color channels; Version 3.2; Carl Zeiss, Inc.) and Photoshop CS2 (brightness and contrast adjustments, cropping; Adobe).²⁴

Endurance exhaustive exercise

For endurance exhaustive exercise, 24-week-old mice were acclimated to and trained on a 10° uphill treadmill (Columbus Instruments) for 2 days. On Day 1, mice ran for 5 min at 8 m/min and on Day 2 mice ran for 5 min at 8 m/min followed by another 5 min at 10 m/min. On Day 3, mice were subjected to a single bout of running starting at the speed of 10 m/min.

Forty minutes later, the treadmill speed was increased at a rate of 1 m/min every 10 min for a total of 30 min, and then increased at the rate of 1 m/min every 5 min until mice were exhausted. Exhaustion was defined as the point at which mice spent more than 5 s on the electric shocker without attempting to resume running even if short air puffs and tail tickles with bristle brush were used to remove the mouse from the shocker²⁷.

Acute exhaustive exercise

For acute exhaustive exercise studies (EE), mice were acclimated to and trained on a 10° uphill treadmill (Columbus Instruments) for 3 days. On training Day 1 mice ran for 5 min at 8 m/min, 5 min for 10 m/min followed by another 5 min at 12 m/min. On training Day 2 mice ran 5 min at 8 m/min, 5 min at 10 m/min, 5 min at 12 m/min, 5 min at 12 m/min followed by another 5 min at 15 m/min. On training Day 3 mice ran 5 min at 10 m/min, 5 min at 12 m/min, 5 min at 15 m/min followed by another 5 min at 18 m/min. On running Day 1–3, mice ran 8 min at 10 m/min, 5 min at 15 m/min, 3 min at 16.8 m/min, 3 min at 18.6 m/min, 3 min at 20.4 m/min, 10 min at 21.4 m/min, then increase 1 m/min every 5 min until the mice were exhausted (Fig. S2A). Exhaustion was defined as the point at which mice spent more than 5 s on the electric shocker without attempting to resume running even if short air puffs and tail tickles with bristle brush were used to remove the mouse from the shocker (time to exhaustion of WT mice is 48.5 ± 3.2 min, time to exhaustion of Fis1KO mice is 49.8 ± 3.6 min). Surface body temperature measurements were collected as described in Reference.²⁸

Blood collection and analysis

Blood was drawn from the retro-orbital sinus of WT and EE mice anesthetized with isoflourane using heparinized capillary tubes. Baseline blood draws were performed on 12-week-old mice prior to exercise. Post-Trial blood draws were immediately collected within 10 minutes of completion on the third day of the EE protocol. Final blood draws were performed at 6 days after completion of the EE protocol. The same mouse was sampled for each time point (Baseline, Post-Trial Immediate and Post-Trial Final) then euthanized at the final blood draw. Serum for cytokines and creatine kinase (CK) were tested as described in Reference.²⁸

Statistical Analysis

Independent students' t-test was used for the data collected only from WT and Fis1KO mice. Statistical analysis for multiple comparisons was performed in GraphPad Prism version 6.0 software using a two-way ANOVA on non-matched samples. Data presented as mean \pm SEM. p-values * <0.05 , ** <0.01 and *** <0.001 , **** <0.0001 , if not indicated otherwise.

Supplementary Material

Refer to Web version on PubMed Central for supplementary material.

Acknowledgements

We would like to thank Richard J. Youle's laboratory for skeletal muscle specific deletion Fis1 mice, advise and thoughtful discussions. We would like to especially thank Dr. Youle for proposing this project and scientific

guidance. We thank Dr. Alicia Pickrell for providing fruitful comments and scientific guidance on this project. We thank inGenious Targeting Laboratory (iTL) for generating the Fis1^{fl/fl} mice. We thank Dr. Jennifer Martinez, PhD, of NIEHS for the plasma analysis and the Clinical Pathology Group in the Cellular & Molecular Pathology Group at NIEHS for the CK plasma analysis. We also thank to the animal husbandry staff at NINDS and the staff of the Murine Phenotyping Core Facility at NHLBI and the staff of NHLBI Electron Microscopy Core Facility. This work was supported by the NIH Intramural National Institute of Neurological Disorders and Stroke Intramural Research Program. Z.Z. is supported by the China Scholarship Council (CSC) for Joint PhD for Research Abroad and Fundamental Research Funds for the Central Universities.

Abbreviations

Fis1	mitochondrial fission 1 protein
EEE	endurance exhaustive exercise
EE	acute exhaustive exercise
ATP	adenosine triphosphate
ADP	adenosine diphosphate
Drp1	dynamamin-related protein 1
Mfn1	mitofusin 1
Mfn2	mitofusin2
NADH	reduced form of nicotinamide-adenine dinucleotide
OPA1	optic atrophy1
OXPPOS	oxidative phosphorylation
LC3	microtubuleassociated protein 1 light chain 3

References

- [1]. Youle RJ, van der Blik AM, Mitochondrial fission, fusion, and stress, *SCIENCE* 2012; 337: 1062–5; PMID:22936770;10.1126/science.1219855 [PubMed: 22936770]
- [2]. Wang X, Destructive cellular paths underlying familial and sporadic Parkinson disease converge on mitophagy, *AUTOPHAGY* 2017; 13: 1998–9; PMID:28598236;10.1080/15548627.2017.1327511 [PubMed: 28598236]
- [3]. Cummins N, Tweedie A, Zuryn S, Bertran-Gonzalez J, Gotz J, Disease-associated tau impairs mitophagy by inhibiting Parkin translocation to mitochondria, *EMBO J* 2019; 38 PMID:30538104;10.15252/embj.201899360
- [4]. Triolo M, Hood DA, Mitochondrial breakdown in skeletal muscle and the emerging role of the lysosomes, *ARCH BIOCHEM BIOPHYS* 2019; 661: 66–73; PMID:30439362;10.1016/j.abb.2018.11.004 [PubMed: 30439362]
- [5]. Hoppins S, Lackner L, Nunnari J, The machines that divide and fuse mitochondria, *ANNU REV BIOCHEM* 2007; 76: 751–80; PMID:17362197;10.1146/annurev.biochem.76.071905.090048 [PubMed: 17362197]
- [6]. Elgass K, Pakay J, Ryan MT, Palmer CS, Recent advances into the understanding of mitochondrial fission, *Biochim Biophys Acta* 2013; 1833: 150–61; PMID:22580041;10.1016/j.bbamcr.2012.05.002 [PubMed: 22580041]

- [7]. Yamano K, Fogel AI, Wang C, van der Blik AM, Youle RJ, Mitochondrial Rab GAPs govern autophagosome biogenesis during mitophagy, *ELIFE* 2014; 3: e1612;PMID:24569479;10.7554/eLife.01612
- [8]. Pickrell AM, Youle RJ, The roles of PINK1, parkin, and mitochondrial fidelity in Parkinson's disease, *NEURON* 2015; 85: 257–73;PMID:25611507;10.1016/j.neuron.2014.12.007 [PubMed: 25611507]
- [9]. Twig G, Elorza A, Molina AJ, Mohamed H, Wikstrom JD, Walzer G, et al., Fission and selective fusion govern mitochondrial segregation and elimination by autophagy, *EMBO J* 2008; 27: 433–46;PMID:18200046;10.1038/sj.emboj.7601963 [PubMed: 18200046]
- [10]. Shen Q, Yamano K, Head BP, Kawajiri S, Cheung JT, Wang C, et al., Mutations in Fis1 disrupt orderly disposal of defective mitochondria, *MOL BIOL CELL* 2014; 25: 145–59;PMID:24196833;10.1091/mbc.E13–09–0525 [PubMed: 24196833]
- [11]. Koch A, Yoon Y, Bonekamp NA, McNiven MA, Schrader M, A role for Fis1 in both mitochondrial and peroxisomal fission in mammalian cells, *MOL BIOL CELL* 2005; 16: 5077–86;PMID:16107562;10.1091/mbc.e05–02–0159 [PubMed: 16107562]
- [12]. Kobayashi S, Tanaka A, Fujiki Y, Fis1, DLP1, and Pex11p coordinately regulate peroxisome morphogenesis, *EXP CELL RES* 2007; 313: 1675–86;PMID:17408615;10.1016/j.yexcr.2007.02.028 [PubMed: 17408615]
- [13]. Tieu Q, Nunnari J, Mdv1p is a WD repeat protein that interacts with the dynamin-related GTPase, Dnm1p, to trigger mitochondrial division, *J CELL BIOL* 2000; 151: 353–66;PMID:11038182;10.1083/jcb.151.2.353 [PubMed: 11038182]
- [14]. Koirala S, Bui HT, Schubert HL, Eckert DM, Hill CP, Kay MS, et al., Molecular architecture of a dynamin adaptor: implications for assembly of mitochondrial fission complexes, *J CELL BIOL* 2010; 191: 1127–39;PMID:21149566;10.1083/jcb.201005046 [PubMed: 21149566]
- [15]. Griffin EE, Graumann J, Chan DC, The WD40 protein Caf4p is a component of the mitochondrial fission machinery and recruits Dnm1p to mitochondria, *J CELL BIOL* 2005; 170: 237–48;PMID:16009724;10.1083/jcb.200503148 [PubMed: 16009724]
- [16]. Jofuku A, Ishihara N, Mihara K, Analysis of functional domains of rat mitochondrial Fis1, the mitochondrial fission-stimulating protein, *Biochem Biophys Res Commun* 2005; 333: 650–9;PMID:15979461;10.1016/j.bbrc.2005.05.154 [PubMed: 15979461]
- [17]. James DI, Parone PA, Mattenberger Y, Martinou JC, hFis1, a novel component of the mammalian mitochondrial fission machinery, *J BIOL CHEM* 2003; 278: 36373–9;PMID:12783892;10.1074/jbc.M303758200 [PubMed: 12783892]
- [18]. Gomes LC, Scorrano L, High levels of Fis1, a pro-fission mitochondrial protein, trigger autophagy, *Biochim Biophys Acta* 2008; 1777: 860–6;PMID:18515060;10.1016/j.bbabo.2008.05.442 [PubMed: 18515060]
- [19]. Lee YJ, Jeong SY, Karbowski M, Smith CL, Youle RJ, Roles of the mammalian mitochondrial fission and fusion mediators Fis1, Drp1, and Opa1 in apoptosis, *MOL BIOL CELL* 2004; 15: 5001–11;PMID:15356267;10.1091/mbc.e04–04–0294 [PubMed: 15356267]
- [20]. Yoon Y, Krueger EW, Oswald BJ, McNiven MA, The mitochondrial protein hFis1 regulates mitochondrial fission in mammalian cells through an interaction with the dynamin-like protein DLP1, *MOL CELL BIOL* 2003; 23: 5409–20;PMID:12861026;10.1128/mcb.23.15.5409–5420.2003 [PubMed: 12861026]
- [21]. Loson OC, Song Z, Chen H, Chan DC, Fis1, Mff, MiD49, and MiD51 mediate Drp1 recruitment in mitochondrial fission, *MOL BIOL CELL* 2013; 24: 659–67;PMID:23283981;10.1091/mbc.E12–10–0721 [PubMed: 23283981]
- [22]. Otera H, Wang C, Cleland MM, Setoguchi K, Yokota S, Youle RJ, et al., Mff is an essential factor for mitochondrial recruitment of Drp1 during mitochondrial fission in mammalian cells, *J CELL BIOL* 2010; 191: 1141–58;PMID:21149567;10.1083/jcb.201007152 [PubMed: 21149567]
- [23]. Touvier T, De Palma C, Rigamonti E, Scagliola A, Incerti E, Mazelin L, et al., Muscle-specific Drp1 overexpression impairs skeletal muscle growth via translational attenuation, *CELL DEATH DIS* 2015; 6: e1663;PMID:25719247;10.1038/cddis.2014.595 [PubMed: 25719247]
- [24]. Winter L, Kuznetsov AV, Grimm M, Zeold A, Fischer I, Wiche G, Plectin isoform P1b and P1d deficiencies differentially affect mitochondrial morphology and function in skeletal muscle,

HUM MOL GENET 2015; 24: 4530–44;PMID:26019234;10.1093/hmg/ddv184 [PubMed: 26019234]

- [25]. Lewis MI, Fournier M, Wang H, Storer TW, Casaburi R, Cohen AH, et al., Metabolic and morphometric profile of muscle fibers in chronic hemodialysis patients, *J Appl Physiol* (1985) 2012; 112: 72–8;PMID:22016372;10.1152/jappphysiol.00556.2011 [PubMed: 22016372]
- [26]. Wang X, Pickrell AM, Rossi SG, Pinto M, Dillon LM, Hida A, et al., Transient systemic mtDNA damage leads to muscle wasting by reducing the satellite cell pool, *HUM MOL GENET* 2013; 22: 3976–86;PMID:23760083;10.1093/hmg/ddt251 [PubMed: 23760083]
- [27]. He C, Bassik MC, Moresi V, Sun K, Wei Y, Zou Z, et al., Exercise-induced BCL2-regulated autophagy is required for muscle glucose homeostasis, *NATURE* 2012; 481: 511–5;PMID:22258505;10.1038/nature10758 [PubMed: 22258505]
- [28]. Sliter DA, Martinez J, Hao L, Chen X, Sun N, Fischer TD, et al., Parkin and PINK1 mitigate STING-induced inflammation, *NATURE* 2018; 561: 258–62;PMID:30135585;10.1038/s41586-018-0448-9 [PubMed: 30135585]
- [29]. Ovchinnikov DA, Macrophages in the embryo and beyond: much more than just giant phagocytes, *GENESIS* 2008; 46: 447–62;PMID:18781633;10.1002/dvg.20417 [PubMed: 18781633]
- [30]. Wallimann T, Wyss M, Brdiczka D, Nicolay K, Eppenberger HM, Intracellular compartmentation, structure and function of creatine kinase isoenzymes in tissues with high and fluctuating energy demands: the ‘phosphocreatine circuit’ for cellular energy homeostasis, *BIOCHEM J* 1992; 281 (Pt 1): 21–40;PMID:1731757;10.1042/bj2810021 [PubMed: 1731757]
- [31]. Moghadam-Kia S, Oddis CV, Aggarwal R, Approach to asymptomatic creatine kinase elevation, *Cleve Clin J Med* 2016; 83: 37–42;PMID:26760521;10.3949/ccjm.83a.14120 [PubMed: 26760521]
- [32]. Song M, Franco A, Fleischer JA, Zhang L, Dorn GN, Abrogating Mitochondrial Dynamics in Mouse Hearts Accelerates Mitochondrial Senescence, *CELL METAB* 2017; 26: 872–83;PMID:29107503;10.1016/j.cmet.2017.09.023
- [33]. Zhang ZK, Li J, Liu J, Guo B, Leung A, Zhang G, et al., Icaritin requires Phosphatidylinositol 3 kinase (PI3K)/Akt signaling to counteract skeletal muscle atrophy following mechanical unloading, *Sci Rep* 2016; 6: 20300;PMID:26831566;10.1038/srep20300 [PubMed: 26831566]
- [34]. Howland RH, “I Want a New Drug”: Exercise as a Pharmacological Therapy, *J Psychosoc Nurs Ment Health Serv* 2015; 53: 13–6;PMID:26248288;10.3928/02793695-20150727-03
- [35]. Friden J, Sjoström M, Ekblom B, Myofibrillar damage following intense eccentric exercise in man, *INT J SPORTS MED* 1983; 4: 170–6;PMID:6629599; [PubMed: 6629599]
- [36]. Hough T, ERGOGRAPHIC STUDIES IN MUSCULAR FATIGUE AND SORENESS, *J Boston Soc Med Sci* 1900; 5: 81–92;PMID:19971340; [PubMed: 19971340]
- [37]. Armstrong RB, Mechanisms of exercise-induced delayed onset muscular soreness: a brief review, *Med Sci Sports Exerc* 1984; 16: 529–38;PMID:6392811; [PubMed: 6392811]
- [38]. Xian H, Yang Q, Xiao L, Shen HM, Liou YC, STX17 dynamically regulated by Fis1 induces mitophagy via hierarchical macroautophagic mechanism, *NAT COMMUN* 2019; 10: 2059;PMID:31053718;10.1038/s41467-019-10096-1 [PubMed: 31053718]
- [39]. Pickrell AM, Huang CH, Kennedy SR, Ordureau A, Sideris DP, Hoekstra JG, et al., Endogenous Parkin Preserves Dopaminergic Substantia Nigral Neurons following Mitochondrial DNA Mutagenic Stress, *NEURON* 2015; 87: 371–81;PMID:26182419;10.1016/j.neuron.2015.06.034 [PubMed: 26182419]
- [40]. Barrientos A, Fontanesi F, Diaz F, Evaluation of the mitochondrial respiratory chain and oxidative phosphorylation system using polarography and spectrophotometric enzyme assays, *Curr Protoc Hum Genet* 2009; Chapter 19: t13–9;PMID:19806590;10.1002/0471142905.hg1903s63
- [41]. Birch-Machin MA, Turnbull DM, Assaying mitochondrial respiratory complex activity in mitochondria isolated from human cells and tissues, *Methods Cell Biol* 2001; 65: 97–117;PMID:11381612; [PubMed: 11381612]
- [42]. Chretien D, Bourgeron T, Rotig A, Munnich A, Rustin P, The measurement of the rotenone-sensitive NADH cytochrome c reductase activity in mitochondria isolated from minute amount of

- human skeletal muscle, *Biochem Biophys Res Commun* 1990; 173: 26–33; PMID:2256918; 10.1016/s0006-291x(05)81016-2 [PubMed: 2256918]
- [43]. Qu X, Yu J, Bhagat G, Furuya N, Hibshoosh H, Troxel A, et al., Promotion of tumorigenesis by heterozygous disruption of the beclin 1 autophagy gene, *J CLIN INVEST* 2003; 112: 1809–20; PMID:14638851; 10.1172/JCI20039 [PubMed: 14638851]
- [44]. Schliwa M, Euteneuer U, Bulinski JC, Izant JG, Calcium lability of cytoplasmic microtubules and its modulation by microtubule-associated proteins, *Proc Natl Acad Sci U S A* 1981; 78: 1037–41; PMID:7015328; 10.1073/pnas.78.2.1037 [PubMed: 7015328]
- [45]. Tokuyasu KT, A technique for ultracryotomy of cell suspensions and tissues, *J CELL BIOL* 1973; 57: 551–65; PMID:4121290; 10.1083/jcb.57.2.551 [PubMed: 4121290]
- [46]. Slot JW, Geuze HJ, Cryosectioning and immunolabeling, *NAT PROTOC* 2007; 2: 2480–91; PMID:17947990; 10.1038/nprot.2007.365
- [47]. Griffiths G, Parton RG, Lucocq J, van Deurs B, Brown D, Slot JW, et al., The immunofluorescent era of membrane traffic, *TRENDS CELL BIOL* 1993; 3: 214–9; PMID:14731755; [PubMed: 14731755]
- [48]. Tokuyasu KT, Immunocytochemistry on ultrathin frozen sections, *Histochem J* 1980; 12: 381–403; PMID:7440248; [PubMed: 7440248]

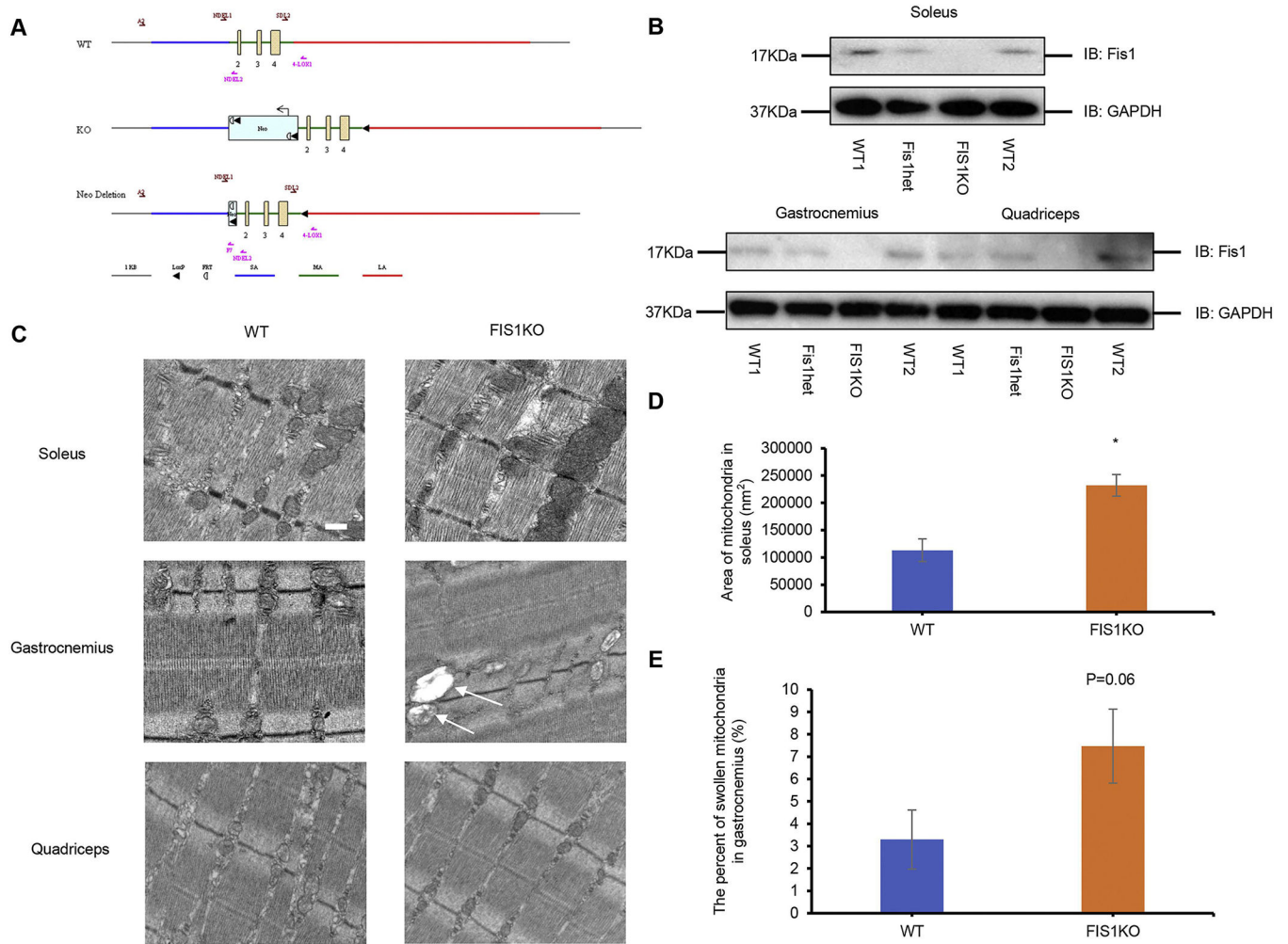


Figure 1. Fis1 deficiency leads to abnormal mitochondrial morphology.

(A) Schematic of gene targeting strategy. LoxP sites and FRT sites flank a splice acceptor site, and neomycin resistance (Neo) cassette. Fis1^{FL/FL} were crossed with MCK-Cre mice (myocyte-restricted (creatine kinase (CK) promoter). (B) Western blots for Fis1 expression. (C) Electron microscopy images of soleus, gastrocnemius and quadriceps (n=3). The arrows indicate the swollen mitochondria (scale bar, 500nm). (D) Statistical evaluation of mitochondrial area as shown in. ** indicates P<0.01. (E) Statistical evaluation of percentage of swollen mitochondria as shown in.

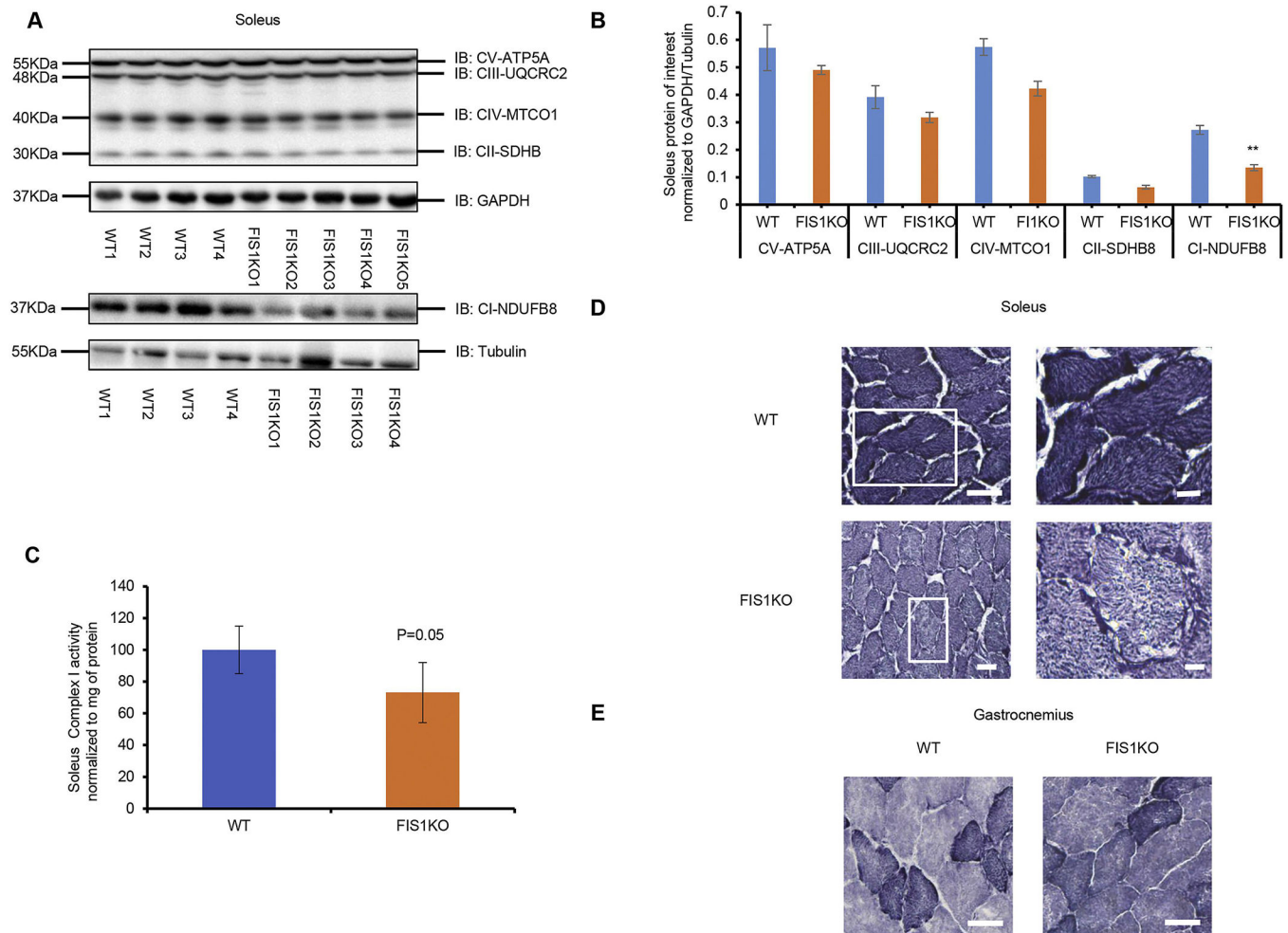


Figure 2. Deletion of Fis1 from myocytes causes reduced expression levels of mitochondrial proteins in Fis1^{-/-}soleus.

(A) Western blots for OXPHOS expression in soleus (n=4–5). (B) Statistical evaluation of OXPHOS expression in soleus as shown in. ** indicates P<0.01. (C) Complex I activity in soleus (n=4–5). (D) Soleus cross-sections obtained from WT and muscle Fis1-deficient (Fis1KO) mice were stained for NADH (n=3) (Scale bar, 50µm). (E) Gastrocnemius cross-sections obtained from WT and muscle Fis1-deficient (Fis1KO) mice were stained for NADH (n=3) (Scale bar, 50µm).

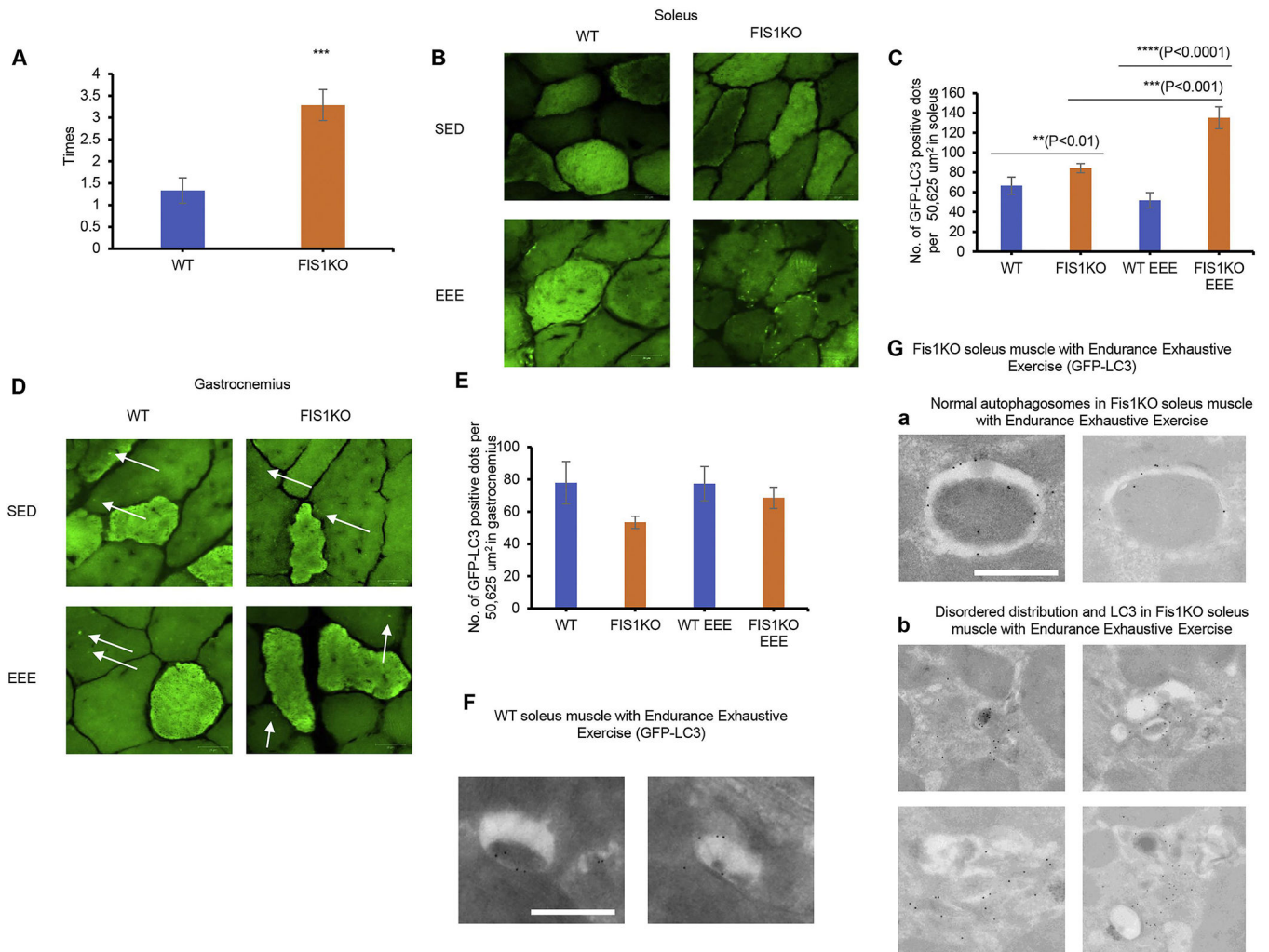


Figure 3. Excessive GFP-LC3 is exacerbated in Fis1-deficient soleus through endurance exhaustive exercise (EEE)
 (A) The performance of treadmill endurance test (n=10–12). (B) Representative images of GFP-LC3 in soleus, (scale bar, 20μm). (C) Statistical evaluation of GFP-LC3 signal in soleus (n=3–4), **, ***, and **** indicates <0.01, <0.001, and <0.0001. (D) Representative images of GFP-LC3 in gastrocnemius, (scale bar 20μm). (E) Statistical evaluation of GFP-LC3 signal in gastrocnemius (n=3–4). (F-G) Immuno-electron microscopy images of WT soleus and Fis1KO soleus following EEE (scale bar, 500nm).

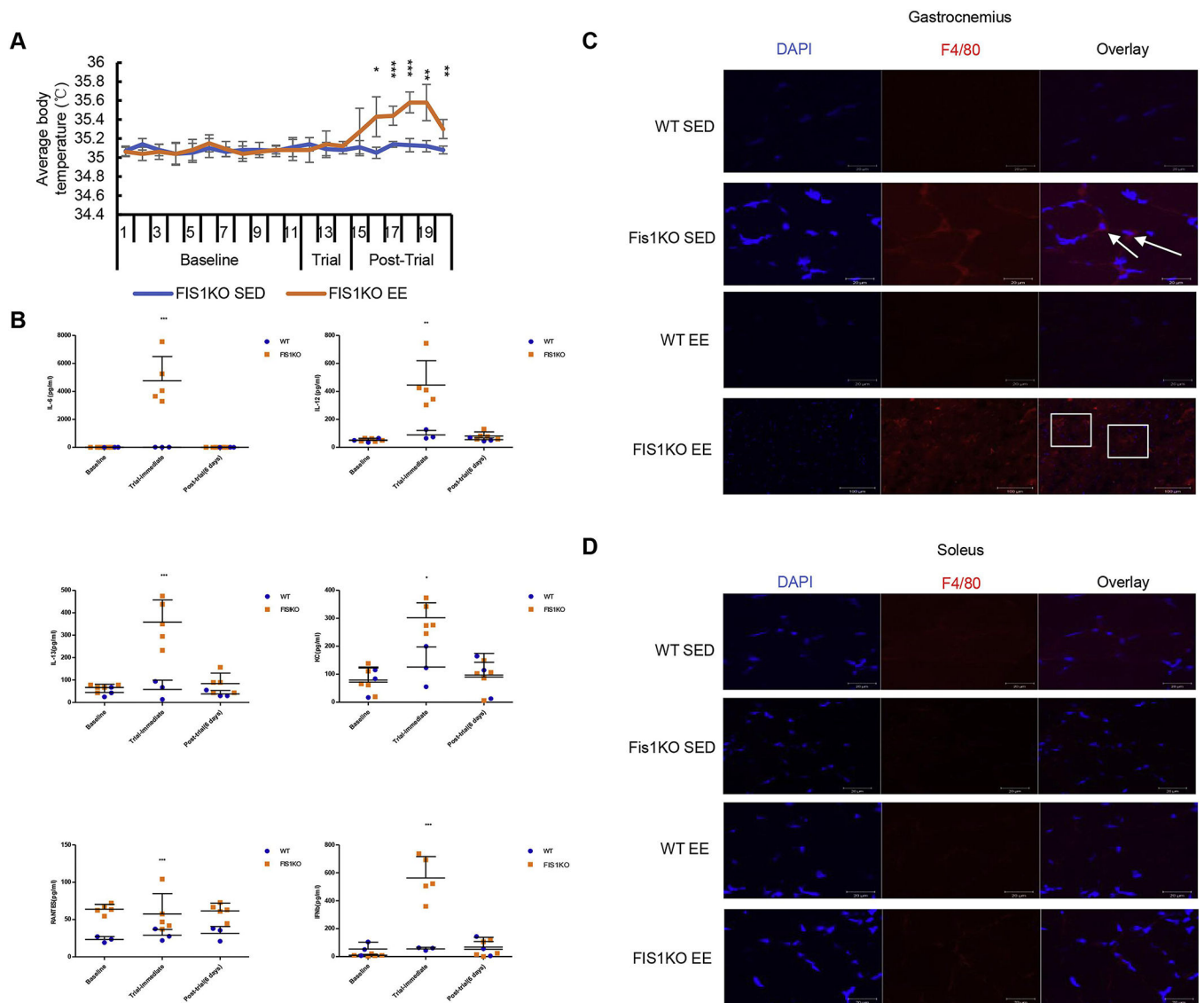


Figure 4. Acute exhaustive exercise exacerbates inflammation response in gastrocnemius and serum.

(A) Average surface body temperature each day of the trial from Fis1KO mice. *, **, and *** indicate <0.05 , <0.01 , and <0.001 ($n=5$). (B) Increased cytokines' level in Fis1KO serum. *, **, and *** indicate <0.05 , <0.01 , and <0.001 ($n=3-5$). (C) Macrophage cells before and after EE in gastrocnemius. (D) Macrophage cells before and after EE in soleus.

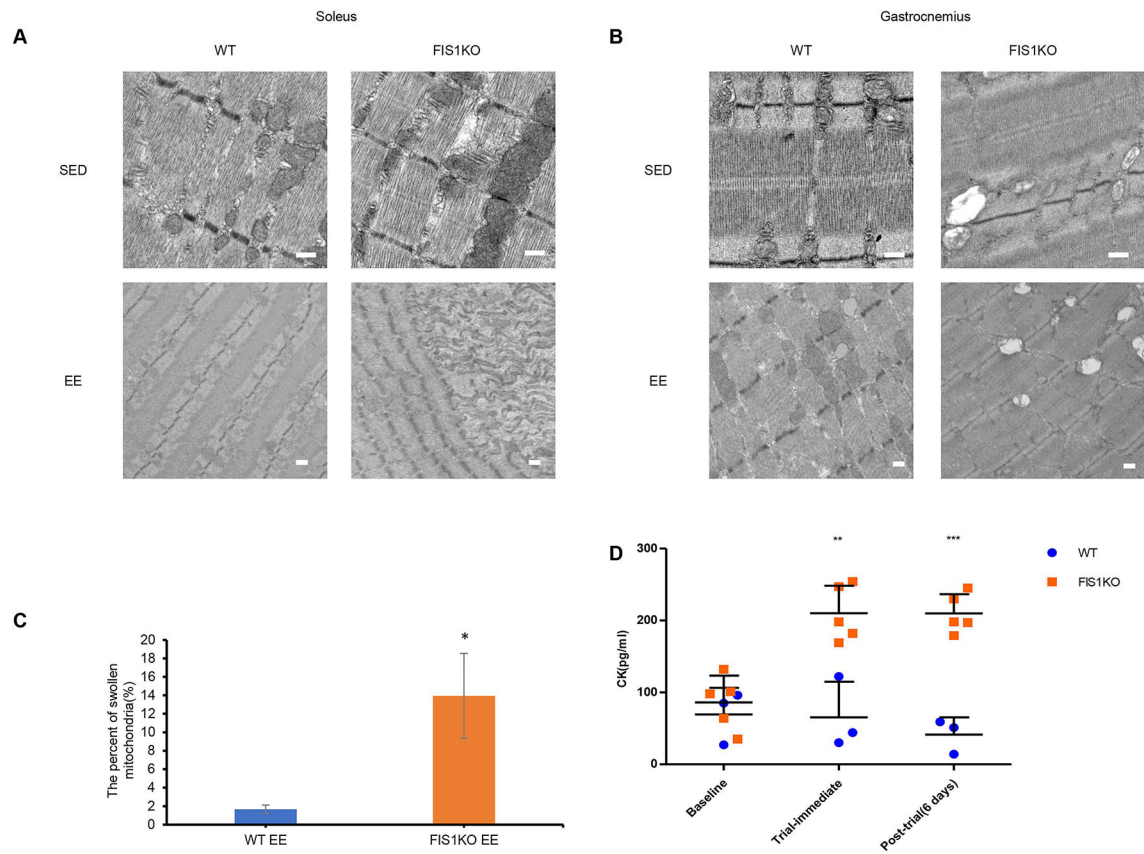


Figure 5. Lack of Fis1 exacerbates DOMS and swollen mitochondria in skeletal muscle after acute exhaustive exercise.

(A) Electron microscopy images of soleus before and after EE (n=3) (Scale bar, 2 μ m). (B) Electron microscopy images of gastrocnemius before and after EE (n=3) (Scale bar, 500nm). (C) Percentage of swollen mitochondria in gastrocnemius before and after EE, * indicates $P < 0.05$ (n=3). (D) Loss of Fis1 leads to persistent high level of creatine kinase in serum after EE. **, *** indicate $P < 0.01, 0.001$ (n=3–5).